Timing of late Quaternary glaciations south of Mount Everest in the Khumbu Himal, Nepal

Ben W.M. Richards
Department of Geography, Royal Holloway, University of London, Egham, Surrey TW20 0EX, UK

Douglas I. Benn*
School of Geography and Geosciences, University of St. Andrews, St. Andrews KY16 9ST, UK

Lewis A. Owen†
Department of Earth Sciences, University of California, Riverside, California 92521, USA

Edward J. Rhodes
Department of Archaeology, Oxford University, Oxford OX1 3PR, UK

Joel Q. Spencer
Department of Earth Sciences, University of California, Riverside, California 92521, USA

ABSTRACT

Moraines south of Mount Everest in the Khumbu Himal were dated using optically stimulated luminescence. Clustering of ages and morphostratigraphy allowed three advances to be dated: (1) the Periche Glacial Stage (ca. 18–25 ka), (2) the Chhukung Glacial Stage (ca. 10 ka), and (3) the Lobuche Stage (ca. 1–2 ka). The Periche Stage is coincident with Oxygen Isotope Stage 2; the Chhukung Stage represents a late glacial or early Holocene glacial advance; and the Lobuche Stage is a late Holocene glacial advance that predates the Little Ice Age.

Keywords: dating, glaciers, Himalaya, Last Glacial Maximum, monsoons, Mount Everest.

INTRODUCTION

The Khumbu Himal is among the most-visited and well-documented regions of the Himalayas, containing three of the world's highest peaks—Mount Everest (Sagarmatha, 8848 m a.s.l. [above sea level]), Lhotse (8501 m a.s.l.), and Cho Oyu (8153 m a.s.l.) (Fig. 1). Several authors (e.g., Iwata, 1976; Fushimi, 1977, 1978; Müller, 1980; Williams, 1983) proposed relative glacial chronologies, although much uncertainty remains concerning the timing and extent of glaciation in this region (Owen et al., 1998). Benn and Owen (1998) emphasized the need for numerical dating of Himalayan glaciations to test the relative importance of the Indian monsoon and midlatitude westerlies in providing moisture and controlling glaciation and hydrology. Elucidating the relative importance of the main climatic forcing mechanisms is essential for reconstructing and modeling paleoenvironmental change in Central Asia during the late Quaternary. In this paper, we provide dates derived from optically stimulated luminescence to determine the timing of glaciations in the Khumbu Himal and to identify the main climatic forcing mechanisms in the Central Himalayas during the late Quaternary.

GLACIAL CHRONOLOGIES

Table 1 summarizes the existing glacial chronologies for the Khumbu Himal and the Rongbuk Valley on the northern slopes of Mount Everest. These glacial chronologies are based on morphostratigraphy and relative weathering criteria. Seven radiocarbon dates have been published for the Khumbu Himal, but all are associated with the most recent (late Holocene) moraines. No organic matter has been recovered from the older moraines. These radiocarbon dates were summarized by Williams (1983) and represent minimum ages for the moraines surrounding the present-day Khumbu and nearby Kyuwo Glaciers (Table 2). For the older moraines, previous workers assigned tentative ages to their chronologies based on the degree of weathering of surface boulders and correlation with the marine oxygen isotopic stages. Such correlation suffers from the assumption that glaciations are synchronous regionally and globally and that relative weathering criteria can be compared directly between and across regions. Gillespie and Molnar (1995) and Benn and Owen (1998) emphasized the possibility that glaciation throughout the Himalayan and Tibetan regions may have been asynchronous. Furthermore, Owen et al. (1997), for example, showed that relative weathering criteria can vary considerably among Himalayan valleys and are only really useful in differentiating moraines within small areas of similar microclimates. Despite these problems, the glacial landforms and successions within the Khumbu Himal can be clearly differentiated and have the potential to be dated by numerical techniques.

*E-mail: doug@st-andrews.ac.uk.
†E-mail: lewis.owen@ucr.edu.

Data Repository item 2000101 contains additional material related to this article.

GSA Bulletin; October 2000; v. 112; no. 10; p. 1621–1632; 7 figures; 3 tables.

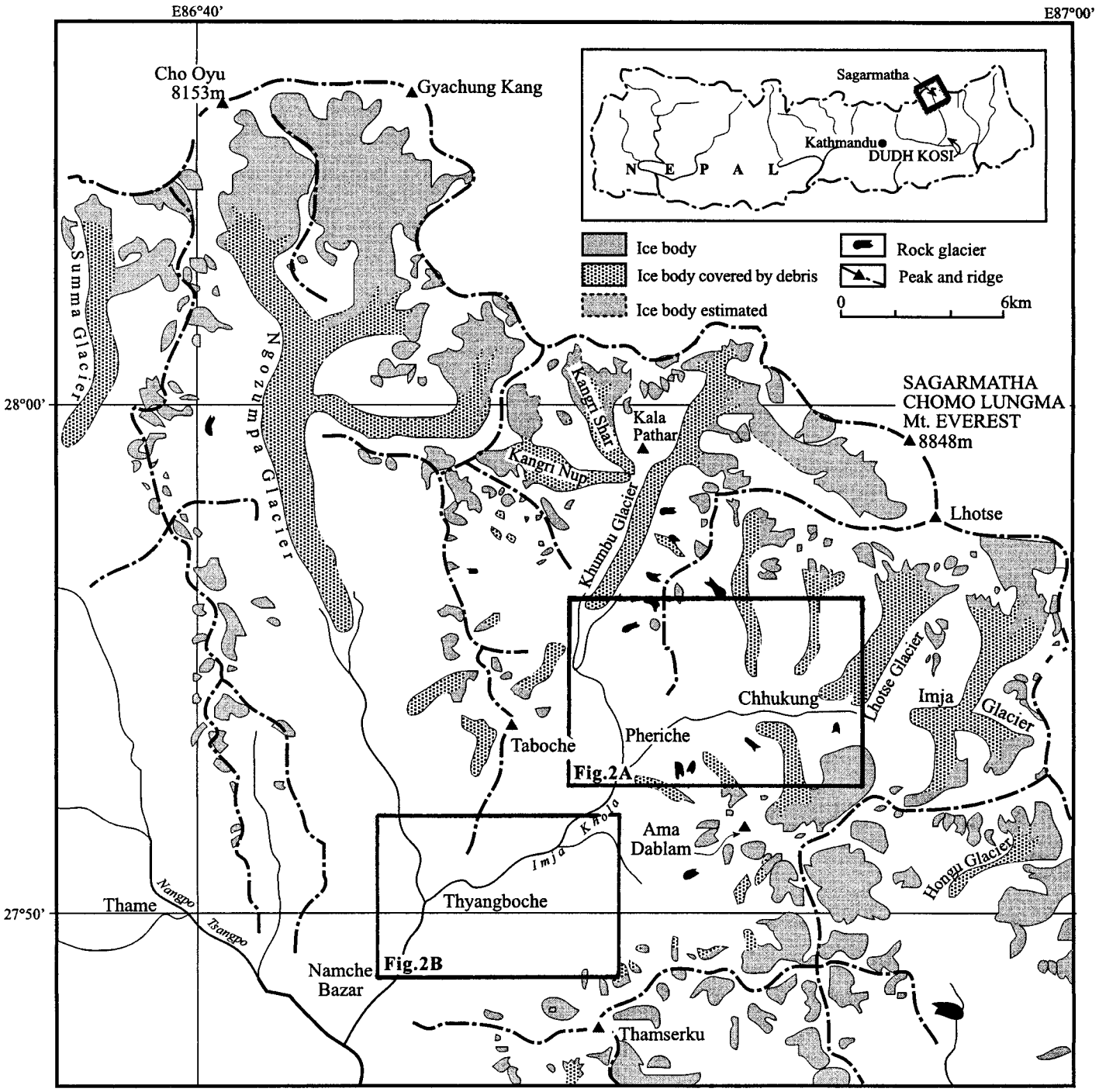

Figure 1. The Khumbu Himal showing the locations of the study areas. The inset boxes show the locations of the detailed maps in Figure 2.

METHODS

Four study areas were chosen to examine the glacial chronologies and to collect sediment samples for dating by optically stimulated luminescence (Figs. 1 and 2). These techniques have been developed during the past two decades to date sediments. Like its precursor, thermoluminescence, optically stimulated luminescence can be used to determine the time elapsed since a sample was exposed to daylight, and has the advantage that bleaching by light is extremely rapid, a 10 s exposure to sunlight resulting in a 99% decrease in luminescence signal of quartz (Godfrey-Smith et al., 1988). Simply explained, the technique relies on the interaction of ionizing radiation with electrons within semiconducting crystals resulting in the accumulation of charge in metastable locations within grains. The population of this charge can be determined by heating (thermoluminescence) or illuminating (optically stimulated luminescence) the grains and detrapping the charge that combines at luminescence centers,

TABLE 1. RELATIVE CHRONOLOGIES FOR KHUMBU HIMALAYA AND TENTATIVE CORRELATIONS, SHOWING THE SAMPLE COLLECTED AND AGES OBTAINED IN THIS PROJECT

Tentative age assigned by previous workers (ka)	Iwata (1976)	Fushimi (1977)	Williams (1983)	Burbank and Kang (1991)	Sampled for this project	OSL ages for this study (ka)
	Khumbu and Imja Valleys	Khumbu and Imja Valleys	Dudh Khunda (south of Imja Valley)	Rongbuk Valley (north of range)	Khumbu and Imja Valleys	Khumbu and Imja Valleys
Late Holocene	Lobuche I–III	Thuklha 3–4	Yykugikcga I–III	Neoglacial	SK06	1.1 ± 0.2
					SK08	2.5 ± 0.4
<5	Thuklha	Thuklha 1	Tamba	Qomolongma II	SK04	9.9 ± 1.8
					SK04*	10.1 ± 1.5
					SK05	9.3 ± 1.8
					SK13	10.9 ± 2.4
ca. 20	Periche	Periche	Lhaog	Qomolongma I	SK09	21.9 ± 3.0
					SK10	24.0 ± 2.8
					SK10*	18.7 ± 5.6
					SK14	21.8 ± 3.9
					SK16	21.3 ± 2.7
					SK17	24.4 ± 2.5
					SK18	25.3 ± 6.9
					ABU-147	20.5 ± 1.4
ca. 40–50	Thyangboche			Early Pleistocene		
>150	Platform	U1		Penultimate glaciation		
Older		U2–3				

Note: OSL—optically stimulated luminescence.
*Duplicate sample using different mineral fraction.

TABLE 2. UNCALIBRATED RADIOCARBON DATES

Moraine ridge location	Müller (1980) Khumbu Glacier (yr)	Benedict (1976) Khumbu Glacier (yr)	Fushimi (1978) Kyuwo Glacier (yr)
Closest to glacier	480 ± 80	550 ± 85 530 ± 165	410 ± 100
Older ridge outside closest ridge	1150 ± 80	1155 ± 160	1200 ± 100*

Note: From moraine ridges close to modern glaciers in the Khumbu Himalayas (after Williams, 1983).

resulting in the emission of photons (luminescence). Artificially dosing subsamples and comparing the luminescence emitted with the natural luminescence can determine the relationship between radiation flux and luminescence. The equivalent dose (D_E) experienced by the grains during burial therefore can be determined[1]. The other quantity needed to calculate an age is the dose rate, which can be derived from direct measurements or measured concentrations of radionuclides. The age is then derived using the equation

$$\text{Age} = D_E/\text{dose rate}. \quad (1)$$

The quoted errors of one standard deviation include all systematic and random errors. Each measured value contributes an element to the total error. For samples measured in this work, the overall age uncertainty is dominated by uncertainty in the D_E values that are relatively large because of the low signal size from the optically stimulated luminescence and the relatively high degree of variation between aliquots. Further details of the technique can be found in a variety of texts—for example, a detailed account of the technique was provided by Aitken (1998).

Samples were analyzed at Royal Holloway, University of London, and at the University of Aberdeen. Most samples were collected in opaque plastic tubes and placed into a light-proof bag that remained sealed until opened under controlled laboratory lighting. Sample SK10 was collected as an intact block, and it was stored in a light-proof bag. The coarse-grained (90–125 μm) quartz fraction was prepared using the standard procedure of Rhodes (1988), with an additional step of 6–8 days immersion in concentrated fluorosilicic acid (H_2SiF_6) following treatment in 40% hydrofluoric acid (HF). The fluorosilicic acid treatment dissolves the remaining feldspars while preserving the quartz. Standard preparation procedures for fine grains (4–11 μm) were used following the methods of Zimmerman (1967). Fine-grained samples were treated subsequently with fluorosilicic acid for 6–7 days to yield fine-grained quartz following the procedures of Rees-Jones (1995). Fine grains of quartz were settled onto aluminum discs from acetone.

All luminescence measurements were made using an automated Risø reader, TL-DA-12, fitted with infrared emitting diodes providing stimulation at 880 ± 80 nm and a filtered halogen lamp as a green light source, which provides broad-band stimulation wavelengths between 420 and 560 nm (2.9–2.2 eV). Emissions were filtered with 5-mm-thick Hoya U340 and 1-mm-thick Schott BG39 glass filters. This arrangement optimizes the detection of luminescence from quartz.

Preliminary equivalent dose (D_E) estimates were determined using the single-aliquot method. Subsequently, 24 to 48 aliquots were measured at eight dose points with the maximum additional beta dose being four to five times the estimated D_E value. All D_E values were determined using a naturally normalized total-integral, multiple-aliquot, additive-dose technique, fitting a single saturating exponential function. Subtraction of the background luminescence signal was by the last-integral subtraction method (Aitken and Xie, 1992). The preheat treatment used for all samples was 220 °C for 5 min. Measurement of all subsamples was carried out, both infrared (infrared stimulated luminescence) and green light (optically stimulated luminescence) for 25 or 50 s of stimulation at room temperature.

The magnitude of a thermal transfer component in the optically stimulated luminescence signal in quartz was determined using a regenerative X-axis intercept (Huntley et al., 1993; Ollerhead et al., 1994;

[1]GSA Data Repository item 2000101, graphic representation of data, is available on the Web at http://www.geosociety.org/pubs/ft2000.htm. Requests may also be sent to Documents Secretary, GSA, P.O. Box 9140, Boulder, CO 80301; E-mail: editing@geosociety.org.

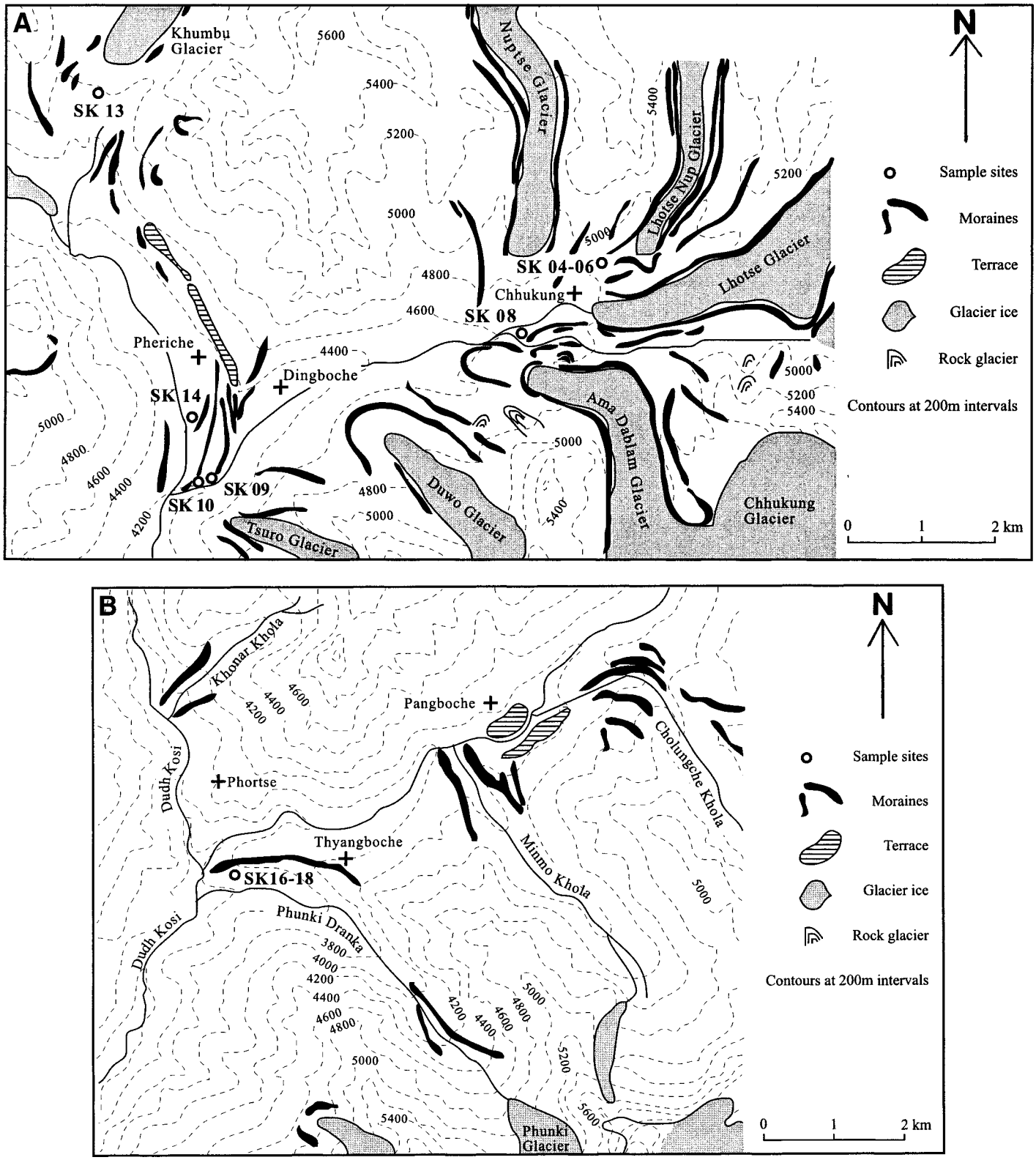

Figure 2. Geomorphic maps showing the main glaciers, moraines, and sampling locations for (A) the Lhotse Nup terminus, the Lhotse moraine, the Dingboche and Periche area, and the Khumbu Glacier study areas; and (B) the Thyangboche study area.

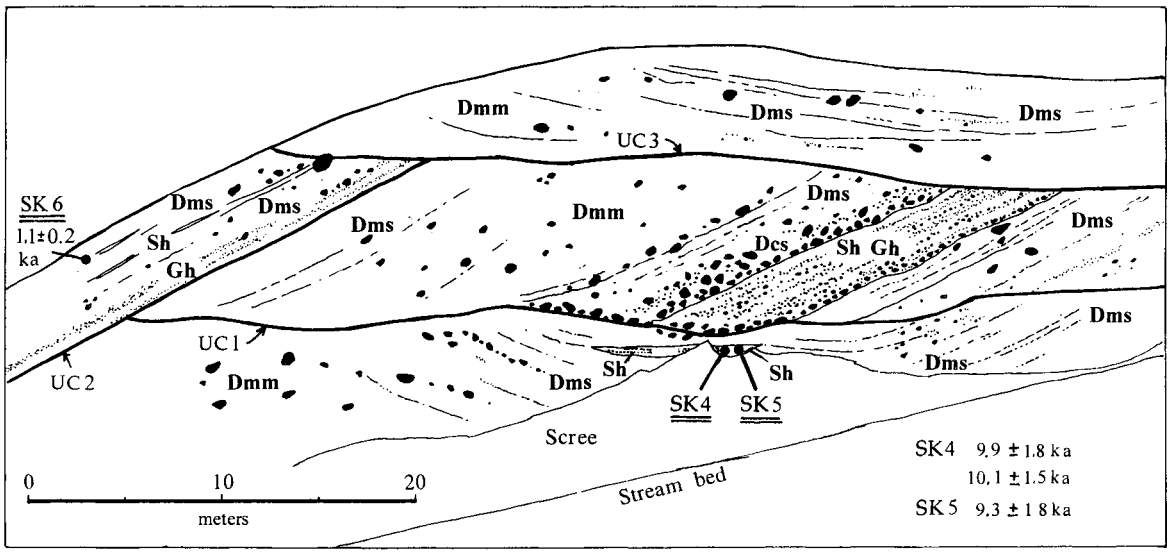

Figure 3. Measured drawing (not to vertical scale) of the Lhotse-Nup section, showing the locations of samples SK4, SK5, and SK6. The section location is shown in Figure 2A. The lithofacies codes of Eyles et al (1983) are used to describe the sedimentology (Dmm—massive matrix-supported diamict; Dms—stratified, matrix-supported diamict; Dcs—stratified, clast-supported diamict; Sh—low-angle, cross-stratified, very fine to very coarse sands; Gh—horizontally bedded gravels). UC1, UC2, and UC3 represent three unconformities.

Figure 4. Photograph of the Lhotse-Nup section, showing the locations of SK4, SK5, and SK6. The south face of Lhotse dominates the background. The relative relief in this photograph is approximately 3700 m.

Rhodes and Bailey, 1997). In all cases, the magnitude of the thermal transfer signal was found to be insignificant.

The environmental dose rate was calculated from neutron-activation analysis of U, Th, and K content of each sample. The cosmic dose rate was calculated according to Prescott and Hutton (1994), based on the present-day depth of overburden and the latitude and altitude of each sample location. The water content was measured by mass lost following drying at 60 °C for each sample. This was used to calculate environmental radiation attenuation during burial.

A duplicate sample for SK09 (ABU-147) was analyzed at the University of Aberdeen as a test of the reliability of the techniques employed for optically stimulated luminescence. Standard procedures were used to prepare a 90–125 μm grain-size fraction of K-feldspar. Measurements made by infrared stimulated luminescence employed a TL-DA-12 Risø reader similar to the system described previously but utilized a combination of Schott BG39 and Corning 7–59 filters for signal detection. The equivalent dose was estimated using a multiple-aliquot additive-dose methodology. A 0.5 s short shine of natural infrared stimulated luminescence at 40 °C (for data normalization) was followed by additive beta doses, preheating at 220 °C for 10 min, and followed by a 200 s shine down of infrared stimulated luminescence at 40 °C. The last-integral technique of Aitken and Xie (1992) was used for background subtraction, and the growth in luminescence fitted well to a linear relationship. A two month fading test showed negligible loss in signal. The environmental dose rate was estimated using a combination of thick-source beta counting, thick-source alpha counting, flame photometry, and cosmic dose rate assessment (Prescott and Hutton, 1994).

STUDY AREAS AND SAMPLING SITES

Lhotse Nup Terminus, Chhukung

Samples SK04, SK05, and SK06 were collected from a section in a large arcuate ridge ~1 km southwest of the terminus of the Lhotse Nup Glacier (Figs. 2 A, 3, and 4). Iwata (1976) assigned this landform to his Thuklha Stage, which he suggested was Holocene. The section consists of crudely stratified, matrix-supported diamict, interbedded with gravel and sand lenses. Four major stratigraphic units are exposed in the section, separated by erosional unconformities (UC 1–3; Fig. 3). Samples SK04 and SK05 were taken from near the top of the lowermost stratigraphic unit, ~40 cm apart in a horizontal bed of fine-grained sand. Sample SK06 was taken near the top of the exposure, from a small lens of sand. The stratigraphic unit from which this sample was taken overlies unconformity UC2 and is truncated by unconformity UC3. It appears, therefore, to represent the penultimate episode of sediment accumulation at this site.

The diamict facies exposed in the section are interpreted as stacked debris-flow deposits, and the intervening gravel and sand units are

interpreted to have resulted from intermittent deposition in shallow (<<1-m-deep), supraglacial braided streams. The sands that were sampled were probably deposited on and between transverse bars as the stream discharges fell from high to low flows. The character of the deposits and the morphology of the ridge in which they occur are similar to those of lateral-frontal moraine complexes in the European Alps (Humlum, 1978; Small, 1983), the North and South American Cordillera (Clapperton, 1993; Johnson and Gillam, 1995), and the Karakoram Mountains (Owen, 1994). This landform, therefore, is interpreted as a lateral-frontal moraine complex deposited when the Lhotse Nup Glacier occupied a more advanced position. The moraine complex appears to have been active on at least four occasions with intervening periods of erosion or nondeposition. The episodes of aggradation represent periods of glacier advance and/or thickening, and, therefore, positive glacier mass balance. The stratigraphic position of samples SK04 and SK05 indicates that they date from near the end of an early stage in the deposition of this landform. Sample SK06, however, represents a later readvance or thickening of the Lhotse Nup Glacier.

Lhotse Moraine

A 30-m-long and 10-m-wide, hummocky moraine ridge is present ~600–800 m southwest of Chhukung village (Fig. 2A). This moraine was formed by the Lhotse Glacier when it extended approximately 2 km farther down the valley from its present terminus. Iwata (1976) assigned this moraine to the Lobuche Stage, to which he tentatively gave an age of less than 5 ka. It is possible that this moraine correlates with the glacial advances that are radiocarbon dated to 1150 ± 80 yr B.P. (Müller, 1980), 1155 ± 160 yr B.P. (Benedict, 1976), and 1200 ± 100 yr B.P. (Fushimi, 1978) (see Williams, 1983).

A 4-m-high section is exposed along the southern edge of the Lhotse moraine (Fig. 5A). The section consists of diamict units with interbedded sands and gravels interpreted as debris-flow and glaciofluvial deposits. Sample SK08 was collected from a small lens of horizontally bedded sand that was deposited in a shallow (~1-m-deep), braided channel formed in a supraglacial environment as river discharges fell from high to low flows.

Dingboche and Periche Area and the Khumbu Glacier Terminus

South and east of Periche village, a series of moraine ridges trend approximately north-south out of the Khumbu Valley (Figs. 2A and 6). Fushimi (1977) divided these moraines into nine discrete substages, in contrast to Iwata (1976), who had argued that one ridge was older than the others and subsequently had been surrounded by more recent ridges. Despite these different interpretations, both Iwata (1976) and Fushimi (1977) assigned these moraines to the Periche Glacial Stage. The moraines can be traced for a considerable distance up the valley. On the eastern side of the valley near Periche, a broad kame terrace and moraine ridge trend obliquely uphill, terminating close to 5000 m a.s.l. near the Khumbu Glacier terminus. On the western side of the valley, moraine benches occur to the west of the Khumbu terminus, on the western flank of Kala Pathar, and above the junction of the Kangri Shar and Kangri Nup Glaciers (Fig. 1). At the latter two locations, the moraines occur at altitudes of ~5400 m (Fig. 6B).

Sample SK09 was taken from a section at the end of the outermost ridge (Figs. 2A and 5B). The ridge consists of massive, matrix-supported, diamict units containing large subrounded boulders. Sample SK09 was collected from planar-bedded sands that are intercalated between diamict units. Sample ABNU-147 also was collected from this site as a duplicate. The planar-bedded sands were deposited as a channel fill within a supraglacial stream that was ~20 cm deep and ~2 m wide. This landform is interpreted as the oldest lateral moraine of a terminal position of the Khumbu Glacier.

Sample SK10 was collected from a section within a moraine ridge ~500 m down the valley from SK09 (Fig. 2A). Sample SK10 was collected from a small unit of well-consolidated, medium-bedded, medium-grained sands that are interbedded within rounded cobbly gravel (Fig. 5C). The landform is interpreted as a lateral moraine that is slightly younger than the moraine from which SK09 was derived. The sampled sediments are interpreted as glaciofluvial in origin and were deposited within a supraglacial braided stream that was ~40 cm deep and 5 m wide.

Sample SK14 was collected from an exposure in a small hummocky landform between the two largest lateral moraines and located close to the Khumbu River (Fig. 2A). The sample was collected from medium-bedded, coarse- to medium-grained sand. These sands are sandwiched between massive, matrix-supported diamicts that contain abundant subangular cobbles and boulders and underlying beds of gravelly sand, and units of massive, matrix-supported diamicts (Fig. 5D). The sampled sediments are interpreted as glaciofluvial materials deposited in a supraglacial environment as fills in braided channels that were ~30–40 cm deep and ~5 m wide. These channels formed as stream discharges fell from high to low flows before the stream was eventually abandoned. These sediments are interbedded between debris-flow units.

A large, dissected moraine is present at the terminus of the Khumbu Glacier. This moraine rises steeply from the gently inclined Periche valley floor at 4500 m a.s.l. to the debris-covered snout of the Khumbu Glacier at 4900 m a.s.l. (Fig. 2A). Iwata (1976) assigned this moraine to three substages of the most recent Lobuche Stage, which he believed formed during the late Holocene. He also mapped two moraine ridges that flank the main dissected moraines and assigned them to the Thuklha Stage, which he believed was older than 5 ka.

Sample SK13 was taken from approximately the center of the dissected moraine. This diamict unit contains angular cobbles and boulders supported in a matrix of sand and silt intercalated with centimeter-thick, planar-bedded beds of partially consolidated, poorly sorted, coarse-grained sands (Fig. 2A and 5E). Sample SK13 was collected from within the intercalated sands, which are interpreted as glaciofluvial sediments filling decimeter-deep and meter-wide, braided channels that are sandwiched between debris-flow deposits. These channels formed in a supraglacial environment.

Thyangboche Ridge

An ~300-m-high, forested ridge bounds the northern side of the Phunki Drangka Valley at Thyangboche. This prominent ridge trends transversely to the Dudh Kosi (Fig. 2B). The ridge is partially rock-cored but is draped with an extensive cover of bouldery diamict, which forms a sharp-crested sediment ridge above the Thyangboche Monastery. Iwata (1976) considered that this ridge marks the terminal position of an advance of the Khumbu-Imja glacier complex, which predates the Periche Stage (the Thyangboche Stage, Table 1). The planar form of the ridge, however, is more consistent with an origin as a lateral moraine of the Phunki Glacier. This interpretation is supported by the fact that the trunk valley (Imja Khola) has a V-shaped lateral profile up the valley of Thyangboche. This profile contrasts to the parabolic, glacially eroded, lateral profiles of the Phunki Drangka and the valleys above the Periche moraines. Large, paired lateral-moraine ridges occur at the northern ends of the Minmo and Cholungche Valleys, which

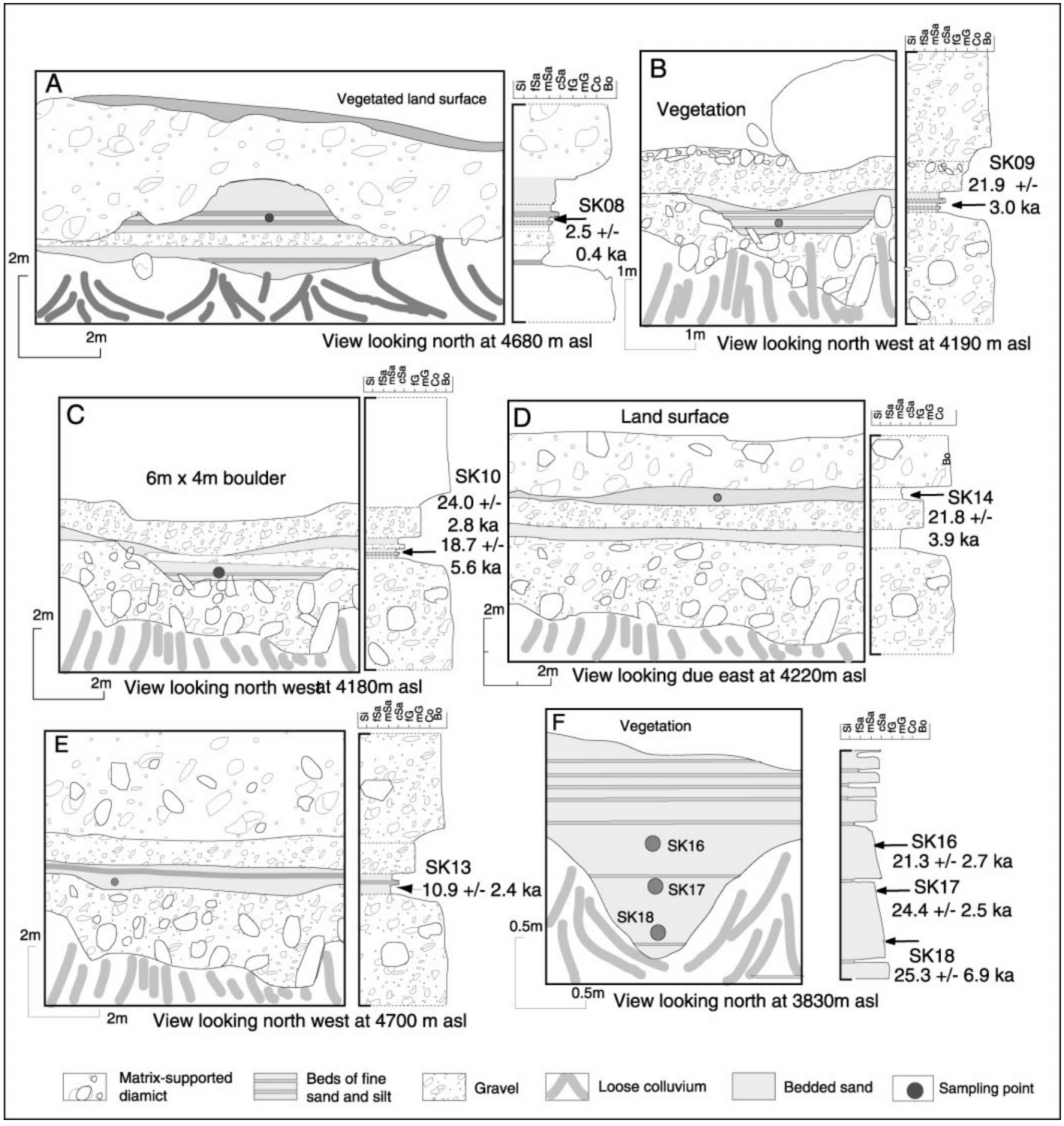

Figure 5. Sections and graphic sedimentary logs showing locations of samples. The section locations are shown in Figure 2. Particle sizes are indicated on the graphic sedimentary logs (sl—silt; fSa—fine sand; mSa—medium sand; cSa—coarse sand; fG—fine gravel; mG—medium gravel; Co—cobbles; Bo—boulders and/or diamict.

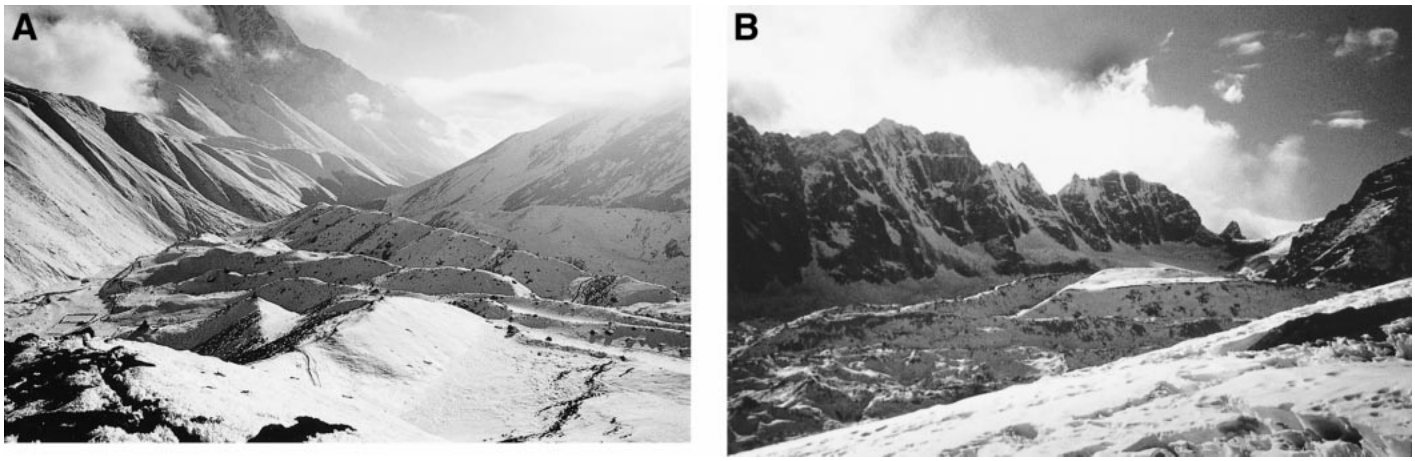

Figure 6. (A) Periche Stage moraines to the south and east of Periche village, looking south. The right lateral moraine is in a shadow on the right, and the left lateral moraines are sunlit or have sunlit crests. The prominent moraines on the left possibly represent equivalent advances of the Churo and Minbo Glaciers that drain Ama Dablam. (B) The junction of the Kangri Nup (left) and Kangri Shar (right) Glaciers viewed from Kala Pathar. The sunlit wedge is a lateral-medial–moraine complex equivalent to the Periche moraines. Also visible are Holocene lateral moraines of the glaciers (possibly Lobuche Stage) and the irregular, debris-covered glacier surfaces.

TABLE 3. INSTRUMENTAL NEUTRON ACTIVATION ANALYSIS, COSMIC DOSE RATE, TOTAL DOSES, AND EQUIVALENT DOSE RATES USED TO CALCULATE LUMINESCENCE AGES

Lab. ID	Type	Sediment			Cosmic dose rate (Gy/yr)	Water content (%)	Total dose rate (Gy/yr)	Equivalent dose (D_E) (Gy)	Age (ka)
		U (ppm)	Th (ppm)	K (%)					
SK04	CGQ	4.91	19.70	3.33	149	6.7	5820 ± 581	57.90 ± 8.90	9.9 ± 1.8
SK04	FGQ	4.91	19.70	3.33	149	6.7	6910 ± 758	70.03 ± 7.08	10.1 ± 1.5
SK05	FGQ	7.43	20.00	4.40	149	2.6	9270 ± 1010	86.29 ± 13.89	9.3 ± 1.8
SK06	CGQ	5.11	19.50	2.82	390	4.2	5780 ± 470	6.3 ± 1.0	1.1 ± 0.2
SK08	CGQ	5.41	21.30	2.55	341	8.6	5390 ± 500	13.6 ± 1.5	2.5 ± 0.4
SK09	CGQ	3.57	12.10	2.26	348	4.0	4288 ± 342	94.08 ± 10.18	21.9 ± 3.0
SK10	CGQ	5.00	20.00	2.91	209	1.1	5912 ± 673	116.55 ± 16.94	24.0 ± 2.8
SK10	FGQ	5.00	20.00	2.91	209	1.1	7130 ± 965	133.53 ± 35.80	18.7 ± 5.6
SK13	CGQ	6.21	15.60	3.38	365	3.5	6313 ± 534	68.66 ± 14.29	10.9 ± 2.4
SK14	CGQ	5.08	16.90	2.50	355	5.0	5112 ± 376	111.49 ± 18.03	21.8 ± 3.9
SK16	CGQ	3.09	13.80	2.66	330	7.9	4460 ± 401	94.76 ± 8.79	21.3 ± 2.7
SK17	CGQ	*	*	*	323	8.0	4520 ± 379	96.20 ± 5.94	24.4 ± 2.5
SK18	CGQ	3.23	11.70	2.96	323	9.5	4520 ± 379	114.60 ± 29.80	25.3 ± 6.9
ABU147	CGF	†	†	†	331	5.0	4470 ± 220†	94.05 ± 3.88	20.5 ± 1.4

Notes: FGQ—fine-grained (4–15 μm) quartz optically stimulated luminescence (OSL), CGQ—coarse-grained (90–125 μm) quartz OSL, and CGF—coarse-grained (90–125 μm) K-feldspar infrared stimulated luminescence. Data and graphic representation of data used to calculate equivalent dose rates (D_E) can be found in the GSA Data Repository. Uncertainties on instrumental neutron activation analysis (INAA) analyses of U, Th, and K are taken to be 10%. The sample numbers SK04–SK18 are the numbers used in the laboratory archive at Royal Holloway, University of London. The sample number ABU147 is from the University of Aberdeen laboratory and is a duplicate sample of SK09.

*No INAA results for SK17. This calculation uses the figures for SK18 because these two samples were from the same thick sedimentary bed, whereas SK16 was collected from a separate bed.

†Estimates from thick source beta counting; gamma calculated from alpha counting and K_2O assessment.

enter the Imja Khola above Thyangboche. These moraines occupy similar topographic positions to the Thyangboche ridge and are probably of similar age.

Samples SK16, SK17, and SK18 were collected from a series of upward-fining beds of coarse- to medium-grained sands exposed on the southern flank of the Thyangboche ridge, ~80 m below its crest. Each upward-fining unit is 4–15 cm thick and is capped by several millimeters of laminated fine-grained sand and silt (Fig. 5F). Some of the fine-grained sand units exhibit ripple cross lamination, and overturned convolute lamination occurs locally at the junction between the graded units and the overlying laminae. The beds dip gently (<10°) toward the south away from the axis of the main ridge. The deposits are interpreted as the products of low-density underflows (turbidites) deposited in a pond or small lake formed against the Thyangboche ridge by glacier ice (cf. Benn and Evans, 1998).

OPTICALLY STIMULATED LUMINESCENCE DATES

Table 3 presents the results of the dates derived from optically stimulated luminescence. The ages cluster into three groups: (1) ca. 18–25 ka, (2) ca. 10 ka, and (3) ca. 1–2 ka. The following five lines of evidence support the reliability of these age data. (1) The ages of the duplicate samples are similar—e.g., SK04 and SK05, collected less than 30 cm apart. (2) The ages have stratigraphic consistency—e.g.,

SK18, SK17, and SK16 (Fig. 5F), which show progressively younger ages, although the errors overlap. (3) The analysis of coarse- and fine-grained quartz fractions provides similar ages on the same samples. (4) The duplication of SK09 (ABU-147) in two laboratories, using both coarse-grained quartz and coarse-grained K-feldspar, produced similar dates. (5) The clustering of ages is consistent with the morphostratigraphic and relative weathering ages on the moraines that were examined. We believe that the degree of internal consistency lends strong support to the interpretation of a high degree of validity to these dates. Rhodes and Bailey (1997) showed that there was potential for dating quartz glaciofluvial samples, provided account was made of the thermal transfer component, which was very large for their samples (on the order of 10 Grays [Gy], i.e., around 10–20% of the D_E values gained in this study). Tests were undertaken to investigate the magnitude of the thermal transfer component in every quartz sample measured for this paper, and it was found to be insignificant. This leads us to expect any age overestimates due to partial bleaching to be not more than around a couple of thousand years. Furthermore, the two very young ages estimates, 1.1 ka and 2.5 ka, indicate that these samples, at least, were well bleached at deposition and provide us with further confidence that the samples that were dated were adequately bleached.

Adequate bleaching of these samples may be due to the fact that Himalayan valley glaciers transport sediment supraglacially and deposit by subaerial processes. This is unlike many high-latitude glaciers in which sediment transport occurs predominantly by subglacial pathways either by basal ice, subglacial till, or meltwater conduits. Therefore, such glacial and glaciofluvial sediments are poorly suited to luminescence dating due to a low probability that they are exposed to sunlight during transport and deposition. All the samples described in the present paper were taken from stratified sediments in lateral-frontal moraine ridges, similar to those found around modern Himalaya valley glaciers. Such ridges are constructed by the deposition of mass-movement and fluvial sediments in ice-marginal aprons fed from supraglacial sources (Owen, 1994). Sediment falls or is carried from the ice surface onto the ice-distal face of the aprons, which prograde through time, creating an outward-dipping structure. On Himalayan valley glaciers, the sediment that feeds ice-marginal moraines is largely of supraglacial origin and follows predominantly supraglacial transport paths. Furthermore, most of the sediments that were dated in this study were collected from shallow (<50-cm-deep), braided-channel fills that were deposited as stream discharges dropped from high to low flows late in the stream's history. Sediment making up such settings will have had a high chance of prolonged exposure to sunlight during entrainment, transport, and deposition and thus would have been bleached prior to deposition. The samples dated in the present study are therefore unlikely to have been only partially bleached.

DISCUSSION AND CONCLUSIONS

The clustering of dates obtained from optically stimulated luminescence suggests that the dated moraines represent three periods of glacial expansion at (1) ca. 18–25 ka, (2) ca. 10 ka, and (3) ca. 1–2 ka.

The earliest of these events has been termed the Periche Glacial Stage (Iwata, 1976; Fushimi, 1977) and correlates with Oxygen Isotope Stage 2. This event is thus coincident with the Last Glacial Maxima of the Laurentide and Eurasian Ice Sheets and local glaciers throughout the northern midlatitudes. The available dates and the morphostratigraphic similarity of the moraines at Thyanboche, Minmo, Cholungche, and Khonar (Fig. 2B) indicate that, at the Last Glacial Maximum, the Khumbu and Imja Glaciers advanced to their confluence, whereas glaciers in the major side valleys lower down the Dudh Kosi catchment reached as far as the trunk valley.

The dating evidence therefore indicates that glaciers in the Khumbu were relatively restricted in extent during Isotope Stage 2. The maximum altitude of lateral moraines of the Periche Stage is ~5400 m, providing a minimum estimate of the equilibrium-line altitude of the Khumbu Glacier at that time (cf. Lichtenecker, 1938; Meierding, 1982; Benn and Lehmkuhl, 2000). The present, steady-state, equilibrium-line altitude of the Khumbu Glacier lies between 5600 and 5700 m (Inoue, 1977; Müller, 1980), so that the Periche Stage moraines represent a lowering of the equilibrium-line altitude of ~200–300 m relative to the present. This lowering agrees with estimates of a depression of the equilibrium-line altitude for Isotope Stage 2 compared with other areas in the Northern Hemisphere and may reflect tectonic uplift and/or climatic factors. Estimates of uplift rates throughout the Himalayas fall in the range of 0.1–1.5 mm/yr (Iwata, 1987; Owen and Derbyshire, 1993), yielding cumulative uplift of only 2–30 m over the last 20 ka. Although uplift rates during the Holocene are poorly known, the available data suggest that uplift is unlikely to explain the relatively low depression of the equilibrium-line altitude for the Khumbu Glacier and that climatic factors were probably more important. The role of climate is discussed in subsequent paragraphs.

The second glacial event that is dated at ca. 10 ka represents a late glacial or early Holocene advance. It is too young to be correlated with the Younger Dryas Stage that has a calendar age of 11.6–12.9 ka B.P. Paleoclimatic records from several regions adjacent to the Himalayas contain evidence for a Younger Dryas climatic event. For example, An et al. (1993) argued that the Younger Dryas in central China was characterized by greater seasonality and strengthened summer monsoon circulation, and Kallel et al. (1988) and Kudrass et al. (1991) documented evidence for a Younger Dryas cooling in ocean cores in the western Pacific. Schulz et al. (1998) documented that the Younger Dryas was a period of reduced biologic productivity in the northern Arabian Sea, probably reflecting a reduction in the intensity or a directional shift of the summer monsoon winds with consequent suppression of coastal upwelling. Pollen and coleopteran records indicate that summer and winter mean temperatures to the west of the Himalayas in eastern Europe were 5 and 11 °C lower, respectively, than those of the present (Coope et al., 1998; Isarin et al., 1998). The presence of Younger Dryas climatic signals from regions to the east, south, and west of the Himalayas indicates that fluctuations in precipitation and/or temperature are likely to have been experienced in the Himalayas at that time and that the event may be recorded in the glacial record. It is therefore surprising that no Younger Dryas event is recorded in the glacial record of the Khumbu Himal. The Lhotse-Nup samples that were dated from near the top of a major stratigraphic unit (Fig. 3), however, may represent an extended period of positive glacial mass balances predating 10 ka. This may be coincident with the Younger Dryas Stage, although we have no evidence for the duration of deposition of this unit. We propose the name Chhukung Stage for the event dated by samples SK04, SK05, and SK13 and assign it to a late glacial or early Holocene age.

Samples SK06 and SK08 represent a late Holocene advance at ca. 1–2 ka. It thus appears likely that this moraine correlates with glacial advances radiocarbon dated to 1150 ± 80 yr B.P. (Müller, 1980), 1155 ± 160 yr B.P. (Benedict, 1976), and 1200 ± 100 yr B.P. (Fushimi, 1978). Our results suggest a late Holocene advance that predates the Little Ice Age in the Khumbu. The Little Ice Age advance may be represented by the uppermost stratigraphic unit in the Lhotse-Nup section (Fig. 3) and by small moraines within the Lobuche moraines at

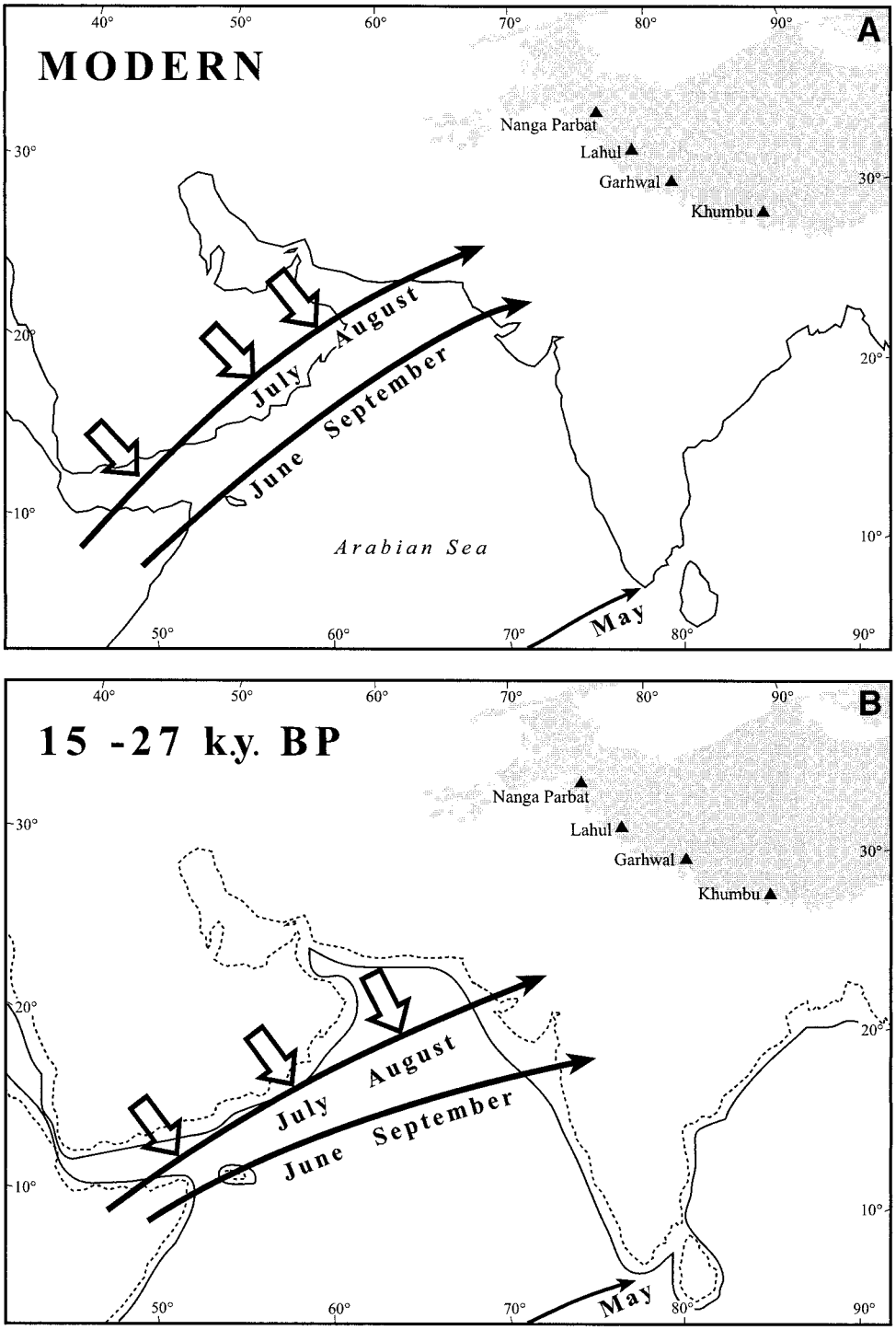

Figure 7. The northernmost frontal position of southwest monsoon winds against northwesterlies during summer for (A) the present and (B) the Last Glacial Maximum (coastline shown at ~100 m below the present). The shaded areas represent areas over 3000 m (Himalayas and Tibetan Plateau). Adapted from Sirocko et al. (1991).

some localities. Testing of this advance and the age of older Holocene moraines and stratigraphic units await further dating studies.

Cosmogenic radionuclide and optically stimulated luminescence dates from the Nanga Parbat region, Pakistan, show that glaciers in that region reached their maximum extent during Oxygen Isotope Stage 3, and that there were less extensive glacial advances during Oxygen Isotope Stage 2 and early to middle Holocene (Sloan et al., 1998; Richards et al., 2000; Phillips et al., 2000). Similarly, Taylor and Mitchell (2000) and Sharma and Owen (1996) obtained dates by means of optically stimulated luminescence indicating that a maximum glacial

advance in Zanskar and the Garhwal Himalaya in India occurred during Oxygen Isotope Stage 3 and with a more restricted glaciation during Oxygen Isotope Stage 2. Iwata (1976) presented evidence for an early, more extensive glaciation, the Thyangboche Glacial Stage, in the Khumbu and Imja Valleys, but this has yet to be numerically dated. However, on the basis of weathering characteristics, Iwata (1976) believed that this glaciation was probably ca. 40–50 ka. Considerable uncertainty exists with the ages of glaciations in these regions because of the limited number of dates presented and the large errors associated with the dating techniques. Nevertheless, from these data it is likely that glaciation throughout the length of the Himalayas was most extensive during the insolation maximum of Oxygen Isotope Stage 3 when the South Asian summer monsoon was strengthened and/or extended its influence further north and west (Clemens et al., 1991; Emeis et al., 1995). Glacial advances during Oxygen Isotope Stage 2 suggest that even though precipitation was probably reduced by comparison to Oxygen Isotope Stage 3, the temperature was sufficiently low to be important as a forcing mechanism in glaciation throughout the Himalayas. Using multiproxy evidence from the Arabian Sea, Sirocko et al. (1991) have argued that during the period 27–15 ka, low-level summer monsoon winds were predominantly west-southwesterlies, rather than the present southwesterlies, and that their influence extended less far to the north and west than at present (Fig. 7). This implies that summer precipitation in the central and eastern Himalayas, such as the Khumbu Himal, may have remained sufficiently high to allow glacier growth during times of regional cooling.

The relatively small amount of lowering of the equilibrium-line altitude on the Khumbu Glacier relative to the present (200–300 m) indicates that the Khumbu region also may have experienced a reduction in precipitation. This could reflect a shortening summer monsoon season consequent upon an overall shift in monsoon circulation (Sirocko et al., 1991, Fig. 7). Moraines relatively dated to Oxygen Isotope Stage 2 in the Rongbuk Valley north of Mountain Everest also indicate small lowering of the equilibrium-line altitude and relative aridity at that time (Burbank and Kang, 1991; Mann et al. 1996).

ACKNOWLEDGMENTS

Three of us—Owen, Rhodes, and Richards—thank the National Environment Research Council for providing financial support for fieldwork and laboratory analysis. Benn thanks Carnegie Trust for financial support to undertake fieldwork in Khumbu. Thanks also are offered to Jim Livingstone, Alison Sandison, and Jenny Johnstone for preparing the photographs and diagrams for publication, and to Douglas H. Clark, Paul Bierman, Steve Forman, and Allen Glazner for their detailed and constructive review of this paper.

REFERENCES CITED

Aitken, M.J., 1998, An introduction to optical dating: Oxford, UK, Oxford University Press, 267 p.

Aitken, M.J., and Xie J., 1992, Optical dating using infrared diodes: Young samples: Quaternary Science Reviews, v. 11, p. 147–152.

An Zhisheng, Porter, S.C., Zhou Weijian, Lu Yanchou, Donahue, D.J., Head, M.J., Wu Xihuo, Ren Jianzhang, and Zheng Hongbo, 1993, Episode of strengthened summer monsoon climate of Younger Dryas age on the loess plateau of central China: Quaternary Research, v. 39, p. 45–54.

Benedict, J.B., 1976, Khumbu glacier series, Nepal: Radiocarbon, v. 18, p. 177–178.

Benn, D.I., and Evans, D.J.A., 1998, Glaciers and glaciation: London, UK, Arnold, 734 p.

Benn, D.I., and Lehmkuhl, F., 2000, Mass balance and equilibrium-line altitudes of glaciers in high mountain environments: Quaternary International, v. 65/66, p. 15–29.

Benn, D., and Owen, L.A., 1998, The role of the Indian summer monsoon and the mid-latitude westerlies in Himalayan glaciation: Review and speculative discussion: Journal of the Geological Society, v. 155, p. 353–363.

Burbank, D.W., and Kang Jian Cheng, 1991, Relative dating of Quaternary moraines, Rongbuk Valley, Mount Everest, Tibet: Implications for an ice sheet on the Tibetan Plateau: Quaternary Research, v. 36, p. 1–18.

Clapperton, C.M., 1993, Quaternary geology and geomorphology of South America: Amsterdam, Netherlands, Elsevier.

Clemens, S., Prell, W., Murray, D., Shimmeld, G., and Weedon, G., 1991, Forcing mechanisms of the Indian Ocean monsoon: Nature, v. 353, p. 720–725.

Coope, G.R., Lemdahl, G., Lowe, J.J., and Walkling, A., 1988, Temperature gradients in northern Europe during the last-glacial–Holocene transition (14–9 ^{14}C kyr B.P.) interpreted from coleopteran assemblages: Journal of Quaternary Science, v. 13, p. 419–433.

Emeis, K.-C., Anderson, D.M., Doose, H., Kroon, D., and Schulz-Bull, D., 1995, Sea-surface temperatures and the history of monsoon upwelling in the northwest Arabian Sea during the last 500,000 years: Quaternary Research, v. 43, p. 355–361.

Eyles, N., Eyles, C.H., and Miall, A.D., 1983, Lithofacies types and vertical profile models, An alternative approach to the description and environmental interpretation of glacial diamict and diamictite sequences: Sedimentology, v. 30, p. 393–410.

Fushimi, H., 1977, Glaciations in the Khumbu Himal: Seppyo, v. 39, p. 60–67.

Fushimi, H., 1978, Glaciations in the Khumbu Himal: Seppyo, v. 40, p. 71–77.

Gillespie, A., and Molnar, P., 1995. Asynchronous maximum advances of mountain and continental glaciers: Reviews of Geophysics, v. 33, p. 311–364.

Godfrey-Smith, D.I., Huntley, D. J., and Chen, W.H., 1988, Optical dating studies of quartz and feldspar sediment extracts: Quaternary Science Reviews, v. 7, p. 373–380.

Humlum, O., 1978. Genesis of layered lateral moraines: Implications for paleoclimatology and lichenometry: Geografisk Tidsskrift, v. 77, p. 65–72.

Huntley, D.J., Hutton, J.T., and Prescott, J.R., 1993, The stranded beach-dune sequence of south-east Australia: A test of thermoluminescence dating, 0–800 ka: Quaternary Science Reviews, v. 13, p. 201–207.

Inoue, J., 1977, Mass budget of Khumbu Glacier: Seppyo, v. 39, p.15–19.

Isarin, R.B.F., Renssen, H., and Vandenberghe, J., 1998, The impact of the North Atlantic Ocean on the Younger Dryas climate in northwestern and central Europe: Journal of Quaternary Science, v. 13, p. 447–453.

Iwata, S., 1976, Late Pleistocene and Holocene moraines in the Sagarmatha (Everest) region, Khumbu Himal: Seppyo, v. 38, p. 109–114.

Iwata, S., 1987, Mode and rate of uplift of the central Nepal Himalaya: Zeitschrift für Geomorphologie, v. 63, p. 37–49.

Johnson, M.D., and Gillam, M.L., 1995, Composition and construction of late Pleistocene end moraines, Durango, Colorado: Geological Society of America Bulletin, v. 107, p. 1241–1253.

Kallel, N., Labeyrie, L.D., Arnold, M., Okada, H., Dudley, W.C., and Duplessy, J.-C., 1988, Evidence of cooling during the Younger Dryas in the western North Pacific: Oceanologica Acta, v. 11, p. 369–375.

Kudrass, H.R., Erlenkeuser, H., Vollbrecht, R., and Weiss, W., 1991, Global nature of the Younger Dryas cooling event inferred from oxygen isotope data from Sulu Sea cores: Nature, v. 349, p. 406–408.

Lichtenecker, N., 1938, Die gegenwärtige und die eiszeitliche Schneegrenze in den Ostalpen, *in* Gotzinger, G., ed., Verhandlungen der III Internationalen Quartar-Conferenz, Vienna, Austria, September 1936: International Quaternary Association, p. 141–147.

Mann, D.H., Sletten, R.S., and Reanier, R.E., 1996, Quaternary glaciations of the Rongbuk Valley, Tibet: Journal of Quaternary Science, v. 11, p. 267–280.

Meierding, T.C., 1982, Late Pleistocene glacial equilibrium-line in the Colorado Front Range: A comparison of methods: Quaternary Research, v. 18, p. 289–310.

Muller, F., 1980, Present and late Pleistocene equilibrium line altitudes in the Mt. Everest region—An application of the glacier inventory: World Glacier Inventory, v. 126, p. 75–94.

Ollerhead, J., Huntley, D.J., and Berger, G.W., 1994, Luminescence dating of sediments from Buctouche Spit, New Brunswick: Canadian Journal of Earth Sciences, v. 31, p. 523–531.

Owen, L.A., 1994, Glacial and non-glacial diamictons in the Karakoram Mountains, *in* Croots, D., and Warren, W. eds., The deposition and deformation of tills: Rotterdam, Netherlands, A.A. Balkema, p. 9–29.

Owen, L.A., and Derbyshire, E., 1993, Quaternary and Holocene intermontane basin sedimentation in the Karakoram Mountains, *in* Shroder, J.F., ed., Himalaya to the sea: Geology, geomorphology, and the Quaternary: New York, Routledge, p. 108–131.

Owen, L.A., Mitchell, W., Bailey, R.M., Coxon, P., and Rhodes, E., 1997, Style and timing of Glaciation in the Lahul Himalaya, northern India: A framework for reconstructing late Quaternary palaeoclimatic change in the western Himalayas: Journal of Quaternary Research, v. 12, p. 83–110.

Owen, L.A., Derbyshire, E., and Fort, M., 1998, The Quaternary glacial history of the Himalaya: Quaternary Proceedings, v. 6, p. 121–142.

Phillips, W.M., Sloan, V.F., Shroder, J.F., Jr., Sharma, P., Clarke, M.L., and Rendell, H.M., 2000, Asynchronous glaciation at Nanga Parbat, northwestern Himalaya Mountains, Pakistan: Geology, v. 28, p. 431–434.

Prescott, J.R., and Hutton, J.T., 1994, Cosmic ray contributions to dose rates for luminescence and ESR dating: Large depths and long-term time variations: Radiation Measurements, v. 23, p. 497–500.

Rees-Jones, J., 1995, Optical dating of young sediments using fine-grain quartz: Ancient TL, v. 13, p. 9–14.

Rhodes, E.J., 1988, Methodological considerations in the optical dating of quartz: Quaternary Science Reviews, v. 7, p. 395–400.

Rhodes, E.J., and Bailey R.M., 1997, Thermal transfer effects observed in the luminescence

of quartz from recent glacio-fluvial sediments: Quaternary geochronology: Quaternary Science Reviews, v. 16, p. 291–298.
Richard, B.W., Owen, L.A., and Rhodes, E.J., 2000, Timing of late Quaternary glaciations in the Himalayas of northern Pakistan: Journal of Quaternary Science, v. 15, p. 283–297.
Schulz, H., von Rad, U., and Erlenkeuser, H., 1998, Correlation between Arabian Sea and Greenland climate oscillations of the past 110,000 years: Nature, v. 393, p. 54–57.
Sharma, M.C., and Owen, L.A., 1996, Quaternary glacial history of the Garhwal Himalaya, India: Quaternary Science Reviews, v. 15, p. 335–365.
Sirocko, F., Sarnthein, M., Lange, H., and Erlenkeuser, H., 1991, The atmospheric summer circulation and coastal upwelling in the Arabian Sea during the Holocene and the last glaciation: Quaternary Research, v. 36, p. 72–93.
Sloan, V., Phillips, W.M., Shroder, J.F., Sharma, P., and Rendell, H., 1998, Asynchronous maximum advances of mountain glaciers in the Pakistan Himalaya: Geological Society of America Abstracts with Programs, v. 30, no. 6, p. 229.
Small, R.J., 1983, Lateral moraines of Glacier De Tsidjiore Nouve: Form, development, and implications: Journal of Glaciology, v. 29, p. 250–259.
Taylor, P.J., and Mitchell, W.A., 2000, The Quaternary glacial history of the Zanskar Range, north-west Indian Himalaya: Quaternary International, v. 65/66, p. 81–100.
Williams, Van S., 1983, Present and former equilibrium-line altitudes near Mount Everest, Nepal and Tibet: Arctic and Alpine Research, v. 15, p. 201–211.
Zimmerman, D.W., 1967, Thermoluminescence from fine grains from ancient pottery: Archaeometry, v. 10, p. 26–28.

MANUSCRIPT RECEIVED BY THE SOCIETY JANUARY 28, 1999
REVISED MANUSCRIPT RECEIVED JANUARY 31, 2000
MANUSCRIPT ACCEPTED JANUARY 31, 2000

Printed in the USA